Original Article

# Amyloid β Protein Aggravates Neuronal Senescence and Cognitive Deficits in 5XFAD Mouse Model of Alzheimer's Disease

**Zhen Wei[1,2,3], Xiao-Chun Chen[1,2,3], Yue Song[1,2,3], Xiao-Dong Pan[1,2,3], Xiao-Man Dai[2,3], Jing Zhang[2,3], Xiao-Li Cui[2,3], Xi-Lin Wu[1,2,3], Yuan-Gui Zhu[2,3]**

[1]Department of Neurology, Fujian Medical University Union Hospital, Fuzhou, Fujian 350001, China
[2]Fujian Institute of Geriatrics, Fujian Medical University Union Hospital, Fuzhou, Fujian 350001, China
[3]Key Laboratory of Brain Aging and Neurodegenerative Diseases, Fujian Key Laboratory of Molecular Neurology, Fujian Medical University, Fuzhou, Fujian 350001, China

## Abstract

**Background:** Amyloid β (Aβ) has been established as a key factor for the pathological changes in the brains of patients with Alzheimer's disease (AD), and cellular senescence is closely associated with aging and cognitive impairment. However, it remains blurred whether, in the AD brains, Aβ accelerates the neuronal senescence and whether this senescence, in turn, impairs the cognitive function. This study aimed to explore the expression of senescence-associated genes in the hippocampal tissue from young to aged 5XFAD mice and their age-matched wild type (WT) mice to determine whether senescent neurons are present in the transgenic AD mouse model.

**Methods:** The 5XFAD mice and age-matched wild type mice, both raised from 1 to 18 months, were enrolled in the study. The senescence-associated genes in the hippocampus were analyzed and differentially expressed genes (DEGs) were screened by quantitative real-time polymerase chain reaction. Cognitive performance of the mice was evaluated by Y-maze and Morris water maze tests. Oligomeric Aβ (oAβ) (1–42) was applied to culture primary neurons to simulate the *in vivo* manifestation. Aging-related proteins were detected by Western blotting analysis and immunofluorescence.

**Results:** In 5XFAD mice, of all the DEGs, the senescence-associated marker p16 was most significantly increased, even at the early age. It was mainly localized in neurons, with a marginal expression in astrocytes (labeled as glutamine synthetase), nil expression in activated microglia (labeled as Iba1), and negatively correlated with the spatial cognitive impairments of 5XFAD mice. oAβ (1–42) induced the production of senescence-related protein p16, but not p53 *in vitro*, which was in line with the *in vivo* manifestation.

**Conclusions:** oAβ-accelerated neuronal senescence may be associated with the cognitive impairment in 5XFAD mice. Senescence-associated marker p16 can serve as an indicator to estimate the cognitive prognosis for AD population.

**Key words:** Alzheimer's Disease; Amyloid β; Cognition; P16; Senescence

## Introduction

Alzheimer's disease (AD) is an age-related dementia, in which the progressive and irreversible memory deficit has afflicted many elderly patients. This disease is pathologically characterized by deposits of amyloid β (Aβ), intracellular neurofibrillary tangles, neuronal and synaptic loss, reactive gliosis, and inflammation.[1] Despite the provision of many hypothesized pathogenic mechanisms, the exact etiological factor and pathogenesis remain poorly understood. As the greatest risk factor for AD, aging has received extensive attention and posed a grave threat to the health-care system,[2,3] but the underlying mechanism of its contribution to cognitive deterioration remains largely unknown.

As one of the hallmarks of aging,[4,5] cellular senescence (CS) not only disrupts the structures of regional tissues and their

Access this article online

Quick Response Code:

Website: www.cmj.org

DOI: 10.4103/0366-6999.186646

**Address for correspondence:** Prof. Xiao-Dong Pan, Department of Neurology, Fujian Institute of Geriatrics, Fujian Medical University Union Hospital, 29 Xinquan Road, Fuzhou, Fujian 350001, China
E-Mail: pxd77316@163.com



**Received:** 21-03-2016 **Edited by:** Xin Chen
**How to cite this article:** Wei Z, Chen XC, Song Y, Pan XD, Dai XM, Zhang J, Cui XL, Wu XL, Zhu YG. Amyloid β Protein Aggravates Neuronal Senescence and Cognitive Deficits in 5XFAD Mouse Model of Alzheimer's Disease. Chin Med J 2016;129:1835-44.

normal function due to its detrimental effects,[6] but also constrains the aberrant progression of tumor cells due to its beneficial effects.[7,8] Besides telomere shortening,[9] cell cycle abnormality such as epigenetic derepression of the INK4a/ARF locus is a key pathological feature for CS,[10] which has crucial implications for aging and age-related degenerative diseases.[11-13] Previous studies have reported the abnormality in the expression of cell cycle-related genes.[14] For example, transformation-related protein 5 (p53), cyclin-dependent kinase inhibitor 1A (p21), and cyclin-dependent kinase inhibitor 2A (p16) have been reported to be closely interconnected with aging and age-related diseases such as AD, diabetes, and cancer. The p16 (INK4a) tumor suppressor accumulates in aging tissues and clearance of p16 (INK4a)-positive senescent cells delays aging-associated disorders.[15] Other studies have verified that p53,[16] cyclin-dependent kinase-4, and its inhibitor p16 were upregulated in AD patients.[17,18] However, this upregulation was based on cross-sectional studies at a single time point, failing to demonstrate the relation between these cell cycle-related genes and cognitive deficits during aging.

With the exciting development in the field, researchers make great efforts to probe into the mechanism of CS in cognitive decline using the rodent model. Early studies have documented that aging and amyloid promote microglial cell senescence and more recent evidence showed that Aβ can promote the senescence of neural stem/progenitor cells in adult mice, affecting forebrain progenitor and hippocampal neurogenesis,[19,20] and can initiate the senescence response in astrocytes recently.[21] However, little attention has been paid to the CS of postmitotic neurons in the aged central nervous system (CNS), which may be related with the severity of cognitive impairments. In the current study, we speculated that Aβ aggravates the CS of the nonglial cells in the brains of 5XFAD mice.

Recently, the importance of neuronal senescence in AD has been a focus in the discussion.[22,23] As a classic transgenic animal model, 5XFAD mice display progressive cognitive decline coupled with Aβ deposition and can be a good model to explore the relationship between aging, Aβ, and cognition.[24] Hence, in this study, we explored the expression of senescence-associated genes in the hippocampal tissue from young to aged 5XFAD mice and their age-matched wild type (WT) mice to determine whether senescent neurons are present in the transgenic AD mouse model.

## Methods

### Animals

Male 5XFAD mice were purchased from Jackson Laboratory (stock no. 034848-JAX, Bar Harbor, ME, USA), which expressed APP K670N/M671L + I716V + V717I and PS1 M146L + L286V under the control of the neuron-specific Thy-1 promoter, resulting in the overproduction of Aβ. These 5XFAD mice and the WT mice were housed under a lighting schedule of 12-h light and 12-h dark (light on at 5:00 am) and allowed free access to water and food. They were classified into 1-month-old groups ($n$ = 6 in each genotype), 3-month-old groups ($n$ = 15 in each genotype), 7-month-old groups ($n$ = 12 in each genotype), 11-month-old groups ($n$ = 10 in each genotype), and 18-month-old groups ($n$ = 9 in each genotype). The age of 5XFAD mice approximated that of WT counterparts in the same age group.

All experiments in this study observed the *Guide for the Care and Use of Laboratory Animals* (NIH Publication, 8th Edition, 2011) and were conducted in accordance with the rules and regulations of the Institutional Animal Care and Use Committee of Fujian Medical University.

### Tissue preparation

After the behavioral tests, animals were anesthetized with 10% chloral hydrate (3 ml/kg) by intraperitoneal injection and perfused with ice-cold 0.1 mol/L phosphate buffer saline (PBS). The brains were rapidly isolated and dissected into halves on ice. The hippocampus of the harvested brains were separated, some were dipped into liquid nitrogen, and stored at −80°C for Western blotting analysis, and others were put in EP tube containing commercial RNA extraction reagent (Roche Applied Science, Indianapolis, IN, USA) for quantitative polymerase chain reaction (qPCR) analysis. The rest of the hemispheres were immersion-fixed in 4% paraformaldehyde at 4°C for 24 h and then dehydrated with 30% sucrose solution twice at 4°C for 48 h. The fixed brains were placed at 4°C in 30% sucrose solution until use.

### Quantitative real-time polymerase chain reaction

The fresh hippocampal tissues were subjected to total RNA extraction using a commercially available assay (Roche) according to the manufacturer's protocol. First-strand cDNA was synthesized with the use of 1 μg of total RNA (Transcriptor First Strand cDNA Synthesis Kit, Roche). The qPCR was performed with Applied Biosystems StepOne (Applied Biosystems, Foster City, CA, USA) using SYBR Green Master (Roche) to measure the fluorescence intensity of amplified products. Reactions were as follows: 55°C for 2 min, 95°C for 10 min, and then 40 cycles of 95°C for 15 s followed by 60°C for 1 min. Data were analyzed by the $2^{-\Delta\Delta Ct}$ method, with glyceraldehyde-3-phosphate dehydrogenase as a housekeeping gene. Fold change of all groups was compared with that of 3-month-old WT group, which was set as one. The sequences of primers are shown in Table 1. All the sequence specificities of the primers used in the current study had been verified by Primer-BLAST (http://www.ncbi.nlm.nih.gov/tools/).

### Western blotting analysis

The hippocampal protein of 5XFAD mice and WT mice was extracted to detect the expression of p53, p21, and p16. For cultured primary neurons, the treated cells were washed with ice-cold PBS, incubated with lysis buffer for 25 min, and then centrifuged to collect the supernatants. Equal amount of proteins (60 μg for brain tissues or 30 μg for cells) was heated at 100°C for 5 min in sodium dodecyl sulfate (SDS) sample loading buffer before being separated

**Table 1: Sequences of primers used for qPCR in this study**

| Murine genes | Forward primer (5'–3') | Reverse primer (5'–3') | Transcripts |
|---|---|---|---|
| Ccnd2 | TCGATGGGCTGCGTTGCGTT | GGGAGCCTGCGTCAAAGGGG | NM_009829 |
| Trp53 | GATGACTGCCATGGAGGAGT | GTCCATGCAGTGAGGTGATG | NM_001127233.1 |
| Cdkn2a | CCCAACGCCCCGAACT | GCAGAAGAGCT-GCTACGTGAA | NM_001040654.1 |
| Cdkn1a | GGCAGACCAGCCTGACAGAT | TTCAGGGTTTTCTCTTGCAGAAG | NM_001111099.1 |
| GAPDH | CAGTGGCAAAGTGGAGATTGTTG | CTCGCTCCTGGAAGATGGTGAT | NM_008084.2 |

qPCR: Quantitative polymerase chain reaction; GAPDH: Glyceraldehyde-3-phosphate dehydrogenase.

by 8% or 10% SDS polyacrylamide gel electrophoresis and transferred to polyvinylidene difluoride membranes at 200 mA for 120 min. The membranes were blocked in 5% nonfat dry milk in Tris Buffered Saline with Tween-20 (TBST) (10 mmol/L Tris, 150 mmol/L NaCl, and 0.1% Tween-20, pH 7.6) at room temperature (RT) for 2 h, and then incubated overnight at 4°C with different primary antibodies: p53 (1:400, Santa Cruz Biotechnology, Dallas, TX, USA), p21 (1:250, Santa Cruz Biotechnology), and p16 (1:1000, Santa Cruz Biotechnology). After three washes with TBST, the membranes were incubated with HRP-conjugated secondary antibody (1:2000, KPL, Gaithersburg, MD, USA) at RT for 90 min. Protein signals were detected with an ECL chemiluminescence substrate reagent kit (Millipore, Billerica, MA, USA) and were quantified with ImageJ software (NIH, Bethesda, MA, USA). The β-actin (1:2000, Abcam, Cambridge, UK) was used as control.

## Immunofluorescence

The hemispheres were sectioned with a freezing microtome (CM1950, Leica, Wetzlar, Germany) and the slices (40 μm in thickness) were stored at −20°C in cryoprotectant solution (30% glycerin, 30% ethylene glycol, and 40% 0.1 mol/L PBS). Immunofluorescence was performed as previously described.[25]

All free-floating tissue sections were pretreated with 0.3 mol/L glycine for 20 min to remove autofluorescence, then washed in Tris-buffered saline (TBS), and blocked with TBS containing 0.3% Triton X-100, 1% BSA, and 5% normal donkey serum (NDS) at RT for 2 h. Slices were then incubated with p16 (1:500, Santa Cruz Biotechnology), NeuN (1:4000, Abcam), glutamine synthetase (GS) (1:4000, Sigma-Aldrich, St. Louis, MO, USA), Iba-1 (1:2000, Wako, Japan), and subsequently with species-specific Alexa secondary antibody (1:1000; Life Technologies, USA), and mounted using prolong Gold antifade reagent (Invitrogen, New York, CA, USA). Confocal images of slides were taken under a LSM 780 META microscope (Carl Zeiss, Oberkochen, Germany). Average fluorescence intensity was measured with Zen software (Carl Zeiss, Oberkochen, Germany).

For cultured primary neurons, the cells were fixed with 4% fresh paraformaldehyde for 25 min before three washes with PBS. After the washes, they were blocked for 1 h with 5% NDS, 0.2% Triton X-100, 0.25% BSA in PBS, and incubated in dilution overnight at 4°C with primary antibodies (p16, 1:500, Santa Cruz Biotechnology; class III β-tubulin, 1:2000, Abcam) and subsequently with a secondary fluorescence Alexa 488 or Alexa 594-conjugated secondary antibody before three washes with Phosphate Buffer Solution with Tween-20 (PBST). Nuclei were counterstained blue with DAPI and coverslipped with prolong Gold antifade reagent (Invitrogen). Images were collected under a confocal laser scanning microscope with different objectives (Zeiss).

## Y-maze test

Spontaneous alternation task was performed as described in a previous study.[26] The Y-maze spontaneous alternation task is based on the fact that rodents have a natural tendency of exploring a novel environment, which need to use visual recognition or spatial working memory, which is hippocampus-dependent. Mice will not likely explore the recently entered arm, and so tend to change visits among the three arms. The Y-maze apparatus was made of Plexiglass and consisted of three identical arms (35 cm × 5 cm × 10 cm) at an angle of 120° with respect to each arm. Except extra-maze cues in the testing room, some specific pattern markers were placed on the walls of the arms to allow for visual distinguishing identifier. Each animal was allowed to explore the entire apparatus freely from the end of one arm for 8 min. The wall and the floor of the Y-maze were sprayed with alcohol after every trial to remove olfactory effect. The sequence and total number of arm entries were recorded by Small Behavioural Video Tracking System (SMART version 2.0, Panlab, Barcelona, Spain). The percentage of spontaneous alteration was calculated by diving the maximum possible alternations (the total number of arm entries −2) with the number of triads containing entries (i.e., 123, 321,…) into all three arms × 100%. In addition, the number of arm entries was regarded as a general indicator of motor activity.

## Morris water maze test

The Morris water maze test was conducted as previously described.[27] Briefly, the black steel pool (120 cm in diameter and 50 cm in height) was filled with water (up to 35 cm in depth and temperature adjusted to 21 ± 1°C). Placed at the center of the Southeast corner was a round platform of transparent plexiglass (10 cm in diameter, 24 cm in height, and about 1.5 cm below the water surface). The RT was also set at 22 ± 2°C by air-conditioning. Some prominent visible cues in the room were used to aid navigation.

During spatial learning training, each mouse undertook four trials per day for 6 consecutive days. Starting from different locations (the north, east, southeast, and northwest, according to semi-random sequence distribution), the mouse

was placed into the water and allowed 60 s to find the hidden platform in each trail. The latency to find the hidden platform within 60 s was recorded for each mouse. If the mouse failed to find the platform within 60 s, it was guided to the platform and allowed to stay there for 15 s and the latency was 60 s. On the 7th day, the platform was removed and a probe trial was conducted. Each animal was allowed to explore the pool freely for 60 s. The computer recorded all performances of the mice (the latency, the swimming orbit, and average distance to the platform in finding the platform, etc.) by the SMART 2.0 video tracking system.

### Primary neuron culture and treatment

Primary neuronal cultures were established from P0 pups of C57BL/6. Briefly, brains from new born mouse pups were dissected and then digested in papain digestion solution (5 U/ml, Worthington Biochemical, Lakewood, CO, USA) at 37°C for 30 min, pelleted, and suspended in neurobasal media. The dissociated cells were equally divided and plated onto coverslips precoated with poly-D-lysine in 24-well plates (Corning, NY, USA) and the coverslips were kept at 37°C in a 95% $O_2$ and 5% $CO_2$ humidified incubator. Neurons were cultured in a complete growth medium containing neurobasal-A (Gibco) media with L-glutamine and 2% B27 (Gibco). Twenty-four hours after seeding, the culture media were changed. Afterwards, the culture media were half changed every 3 days. The neurons were treated with various concentrations (vehicle, 2.5, 5 or 10 μmol/L) oligomeric amyloid β (oAβ) at the 7th day for 4 h or 24 h. The preparation of oligomers by lyophilized Aβ (1–42) peptide (AnaSpec, Fremont, CA, USA) followed the procedures has been described in a previous study.[28]

### Statistical analysis

Data, expressed as mean ± standard error (SE), were derived from at least three independent experiments and analyzed with the GraphPad Prism 6.01 software package (GraphPad, San Diego, CA, USA). Expressions of differentially expressed genes (DEGs) were indicated as relative expression levels using the $2^{-\Delta\Delta Ct}$ method. Normality and homoscedasticity assumptions were reached, validating the application of the two-way analysis of variance (ANOVA; two variables analyzed in all cases). If the main effects and the interaction were significant, Student's *t*-test was used to compare the genotypes or one-way ANOVA was used to compare multiple conditions among the same genotype. Multiple comparisons were analyzed by Bonferroni *post hoc* test. For distance to the platform and escape latency, significance of the main effects and the interaction were evaluated by a repeated measure multi-way ANOVA. Differences were considered statistically significant at $P < 0.05$.

## Results

### Altered profile of cell cycle-related genes in the hippocampus 5XFAD mice

Four key senescence-related genes (cell cycle-related genes *p53*, *p21*, *p16*, and cyclinD2), which are closely associated with aging and AD, were selected for qPCR analysis to screen and quantify DEGs in the hippocampus from 5XFAD and age-matched WT mice. Clearly, cyclinD2 was not obviously changed during the aging course while cell cycle suppressor genes *p53*, *p16*, and *p21* changed to varying degrees in 5XFAD mice. Compared with that of age-matched WT mice, *p53* messenger RNA (mRNA) was transiently and mildly upregulated only in the 7-month-old 5XFAD mice ($t = 2.643$, $P = 0.033$), but no significant differences were found in other age groups. Interestingly, compared with that of age-matched WT mice, *p16* mRNA level in 5XFAD mice increased dozens of times, especially after 7 months (5XFAD vs. age-matched WT: $t = 0.006$, $P > 0.05$ for 1-month-old; $t = 2.237$, $P = 0.045$ for 3-month-old; $t = 4.282$, $P < 0.001$ for 7-month-old; 5XFAD vs. $t = 4.878$, $P < 0.001$ for 11-month-old; and $t = 7.601$, $P < 0.001$ for 18-month-old). The mRNA level of *p21* in 5XFAD mice was not significantly upregulated until 18 months old (5XFAD vs. age-matched WT: $t = 0.233$, $P > 0.05$ for 1-month-old; $t = 0.317$, $P > 0.05$ for 3-month-old; $t = 0.311$, $P > 0.05$ for 7-month-old; $t = 2.246$, $P > 0.05$ for 11-month-old; and $t = 3.687$, $P < 0.01$ for 18-month-old) [Figure 1a].

To further confirm the validity of mRNA changes of *p53*, *p21*, and *p16*, Western blotting analysis was performed simultaneously to detect these protein lysates from the hippocampal tissues of 5XFAD mice and age-matched WT mice. Quantitative results of Western blotting revealed that p16 significantly increased at different ages in the 5XFAD mice (5XFAD vs. age-matched WT: $t = 3.374$, $P < 0.05$ for 3-month-old; $t = 3.454$, $P < 0.05$ for 7-month-old; $t = 3.459$, $P < 0.05$ for 11-month-old; and $t = 4.988$, $P < 0.001$ for 18-month-old) and p21 was upregulated only in the 18-month-old 5XFAD mice (5XFAD vs. age-matched WT: $t = 0.249$, $P > 0.05$ for 3-month-old; $t = 0.107$, $P > 0.05$ for 7-month-old; $t = 1.942$, $P > 0.05$ for 11-month-old; and $t = 3.475$, $P < 0.05$ for 18-month-old), while the protein level of p53 was not significantly different between 5XFAD mice and age-matched WT mice ($t = 0.282$, 0.169, 0.015, and 0.185 from 3-month-old to 18-month-old, respectively, all at $P > 0.05$) [Figure 1b].

### The increased expression of p16 in neurons

To investigate the morphological change of p16 in the hippocampus, we chose young (3 months old) and aged (18 months old) mice as the subjects of study in the single immunofluorescence staining. Compared with age-matched WT mice, the immunofluorescence intensities of p16 in the pyramidal cells of *cornu ammonis 1* (CA1) of young and aged 5XFAD mice were increased by 0.51-fold ($t = 4.056$, $P < 0.01$) and 2.70-fold ($t = 24.690$, $P < 0.001$), respectively [Figure 2a]. The immunoreactivities of p16 in the aged 5XFAD and WT mice were, respectively, increased by 2.86-fold ($t = 17.430$, $P < 0.001$) and 0.59-fold ($t = 6.815$, $P < 0.001$), compared with those of the same genotypes in young mice. Of note, besides CA1 of the hippocampus, similar phenomenon was present in other brain regions such as dentate gyrus (data not shown).

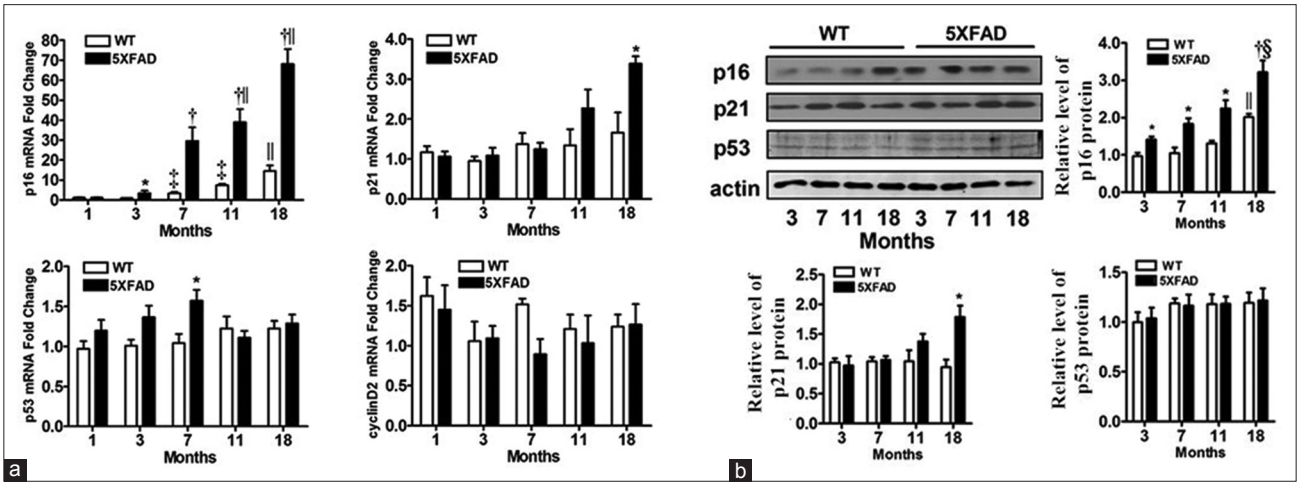


**Figure 1:** Cell cycle-related genes screened in the hippocampus of 5XFAD mice. p16 was significantly upregulated. (a) The mRNA levels of senescence-associated DEGs were measured by qPCR. Among the four DEGs (cell cycle-associated *p53*, *p21*, *p16*, and cyclinD2), the upregulation of *p16* was the most significant change. Data were normalized to the levels of *GAPDH* mRNA and analyzed by Bonferroni *post hoc* test. (b) Representative Western blotting analysis of p53, p21, and p16 in whole hippocampal lysate. Data were normalized to actin and expressed as mean ± standard error. $^{*}P < 0.05$, $^{\dagger}P < 0.001$, compared with age-matched wild type mice; $^{\ddagger}P < 0.05$, $^{\S}P < 0.01$, $^{||}P < 0.001$, compared with the 3-month-old group of the same genotype. DEG: Differentially-expressed gene; *GAPDH*: Glyceraldehyde-3-phosphate dehydrogenase; qPCR: Quantitative polymerase chain reaction; mRNA: Messenger RNA.

To investigate the cell type of p16 expression, double immunofluorescence staining was performed for p16 and different markers of specific cell types. As shown in Figure 2b, neurons of the pyramidal cell layer from the aged 5XFAD mice displayed a rosy co-localization of p16 and neuronal marker NeuN. However, p16 was sparingly expressed in astrocytes labeled with GS, but not in activated microglia when sections were contained with p16 and Iba1 [Figure 2b].

Together, these results suggested that the change of senescence-related protein p16 in hippocampal neurons seemed to be an early event and progressed with the AD development.

## Deteriorated cognitive impairment in 5XFAD mice

To evaluate the cognitive profile of 5XFAD and WT mice, we tested the cognitive performance of mice at different ages with the Y-maze and Morris water maze tests.

The total activity, calculated by the number of total arm entries in the Y-maze test, was not significantly changed among the eight groups despite a decreasing trend in the aged groups, indicating that exploratory activity was not remarkably affected by genotype and aging [Figure 3a]. Notably, compared with the same age of WT mice, 5XFAD mice displayed significantly lower rates of spontaneous alternation performance ($t = 2.592$, $P < 0.05$ for 7-month-old; $t = 3.740$, $P < 0.01$ for 11-month-old; and $t = 3.153$, $P < 0.01$ for 18-month-old) except the 3-month-old groups ($t = 1.102$, $P > 0.05$) [Figure 3b].

To further determine the changes in learning and memory during aging, we examined the performance of all groups in the Morris water maze test, which depends on the hippocampal function and challenges spatial navigation and reference memory. As shown in Figure 3c–3f, the escape latency and the average distance to the platform in every training day were measured.

Multi-way repeated measures ANOVA showed significant main effects of time ($F = 42.60$, $P < 0.001$ for the escape latency; $F = 16.14$, $P < 0.001$ for the average distance), genotype ($F = 8.45$, $P < 0.001$ for the escape latency; $F = 13.03$, $P < 0.001$ for the average distance), and age ($F = 22.01$, $P < 0.001$ for the escape latency, $F = 14.01$, $P < 0.01$ for the average distance) in the training days.

With the increasing training day, the escape latency and the average distance in all groups decreased gradually except in 11- and 18-month-old 5XFAD groups. Compared with the WT mice, the 5XFAD mice showed significant increases in the escape latency and average distance to the platform ($P < 0.01$ or $P < 0.001$) [Figure 3c–3f]. On the basis of learning curve of the escape latency, the approximate order of learning ability from high to low was 3-month-old WT, 7-month-old WT, 3-month-old 5XFAD, 7-month-old 5XFAD, 11-month-old WT, 18-month-old WT, 11-month-old 5XFAD, and 18-month-old 5XFAD.

In the probe trial day, the platform was removed. Compared with WT mice, the 5XFAD mice crossed significantly less over the location of the removed platform ($t = 2.262$, $P < 0.01$ for 3-month-old; $t = 2.923$, $P < 0.01$ for 7-month-old; $t = 3.306$, $P < 0.01$ for 11-month-old; and $t = 2.80$, $P < 0.05$ for 18-month-old) [Figure 3d] and spent less time in the target quadrant ($P < 0.05$ for each age group) [Figure 3e]. Compared with the 3-month-old group, the aged mice showed an obvious decrease in crossing number (5XFAD groups: 3-month-old vs. 7-month-old group, $t = 3.027$, $P < 0.05$; 3-month-old vs. 11-month-old group, $t = 3.620$, $P < 0.01$; and 3-month-old vs. 18-month-old group, $t = 4.066$, $P < 0.01$. WT groups: 3-month-old *vs.*

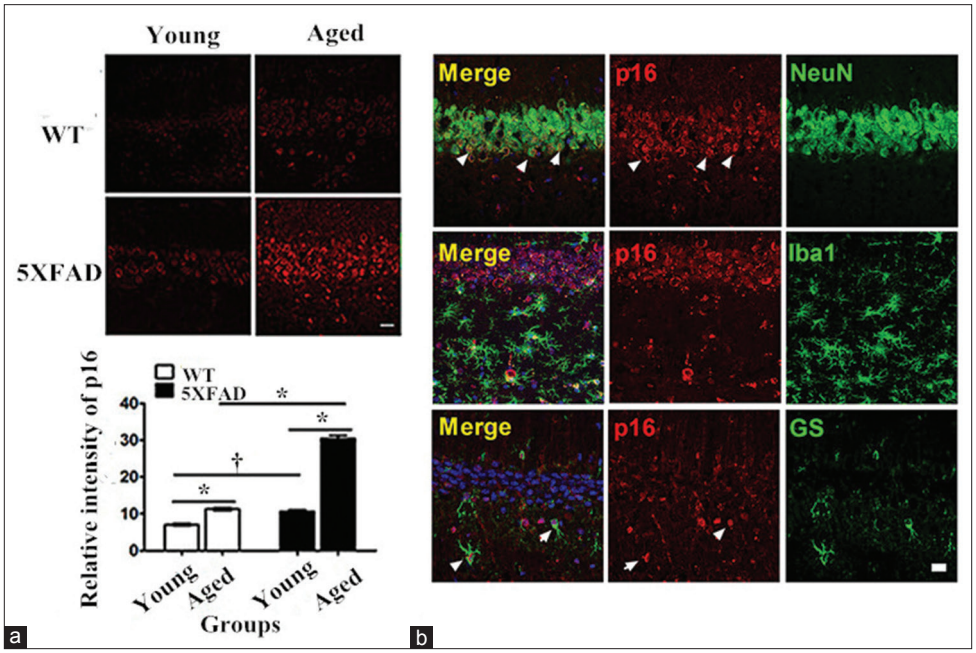


**Figure 2:** Localization and upregulation of senescence-associated marker p16 in neurons under the AD context. (a) Representative confocal photomicrographs of the hippocampal CA1 region. The IR of p16 (red) was increased in pyramidal cells of aged 5XFAD mice. Average fluorescence intensity of p16-IR in the pyramidal cell layer was quantified in the column graph. Data were expressed as mean ± standard error. $^{*}P < 0.001$, $^{\dagger}P < 0.01$. (b) The cellular localization of p16 in the hippocampal CA1 region of brains from aged 5XFAD mice (18-month-old) was investigated by double immunofluorescence staining. Just as white arrows indicated, p16 was mostly co-localized with NeuN (a neuron marker), only marginal expression in GS-positive astrocytes and almost nil expression in Iba-1-positive microglia. $n = 3$ in each group. Scale bar = 20 μm. AD: Alzheimer's disease; IR: Immunoreactivity; GS: Glutamine synthetase.

7-month-old group, t = 0.6133, $P > 0.05$; 3-month-old vs. 11-month-old group, $t = 2.124$, $P > 0.05$; and 3-month-old vs. 18-month-old group, $t = 3.263$ $P < 0.01$) [Figure 3d] and time spent in the target quadrant (5XFAD groups: 3-month-old vs. 7-month-old group, $t = 2.365$, $P > 0.05$; 3-month-old vs. 11-month-old group, $t = 3.423$, $P < 0.01$; and 3-month-old vs. 18-month-old group, $t = 3.731$, $P < 0.01$. WT groups: 3-month-old vs. 7-month-old group, $t = 1.603$, $P > 0.05$; 3-month-old vs. 11-month-old group, $t = 3.154$, $P < 0.05$; and 3-month-old vs. 18-month-old group, $t = 3.312$, $P < 0.05$) [Figure 3e]. The similar phenomenon was also confirmed by the results of distance to platform [Figure 3f].

These results indicated that 5XFAD mice displayed deteriorated cognitive performance. Of note, the 11-month-old and 18-month-old 5XFAD mice performed similarly poorly in the test, indicating a ceiling effect in the cognitive progress profile.

## Significant negative association between *p16* gene expression and cognitive impairment

To explore the role of p16 and p53 in the cognitive impairment during aging, we performed Person's correlation analysis. As shown in Table 2, significant negative correlations were observed between *p16* gene expression and multiple cognitive performances (spontaneous alteration, number of crossings, and time spent in the target quadrant), but not *p53*. To our knowledge, this study revealed an inverse relationship between senescence-associated marker *p16* gene expression and cognitive performance in an AD model during the aging course.

## Amyloid β-facilitated expression of p16 in neurons *in vitro*

5XFAD mice displayed a gradual and rapid Aβ deposition, which is the main pathological feature of AD in the hippocampus. Hence, in the light of the drastically elevated p16 expression in the 5XFAD mice, we speculated whether Aβ exposure would affect the expression level of p16 in cultured neurons.

To confirm this speculation, cultured primary neurons were exposed to oAβ in various concentrations (vehicle, 2.5, 5, or 10 μmol/L) for 4 h and 24 h, and the protein levels of p16 and p53 were detected by Western blotting analysis. Of the various concentrations, the treatment with 10 μmol/L oAβ most effectively upregulated the p16 expression, with an increase to 153 ± 10% 4 h after stimulation ($t = 4.555$, $P < 0.01$) and 197 ± 18% 24 h after stimulation ($t = 7.138$, $P < 0.001$) [Figure 4a]. Notably, the protein expression of p53 in neurons was not significantly changed at both 4 h and 24 h after the oAβ treatment. This finding was consistent with our *in vivo* observation. Alterations of p16 protein in the primary neurons after the oAβ stimulation were further confirmed by immunostaining. As demonstrated by Figure 4b, the immunofluorescence signal of p16 in the nuclear of neurons (βIII-tubulin as a neuronal marker) paralleled the increasing concentration of Aβ.

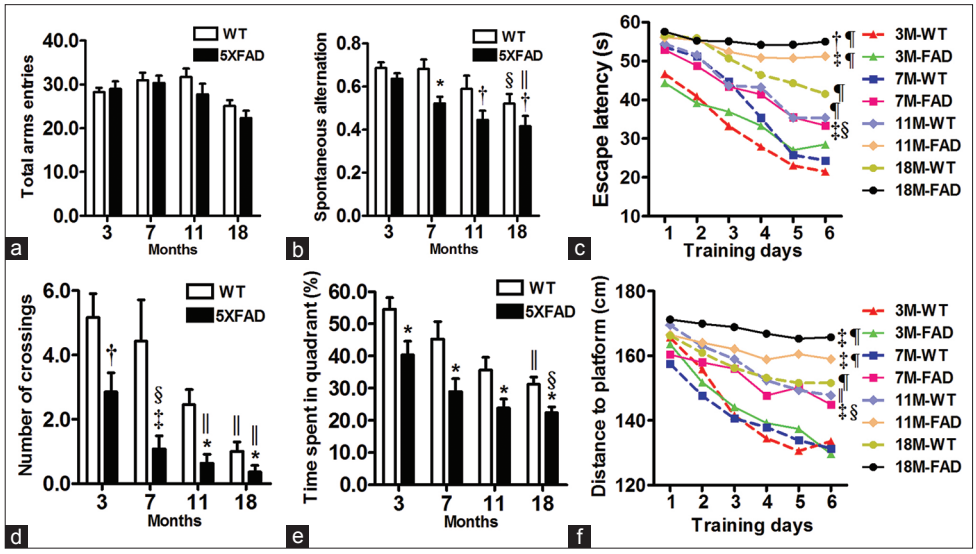


**Figure 3:** Exacerbation of age-dependent cognitive impairment in 5XFAD mice by cognitive-behavioral test. Y-maze (a and b) and Morris water maze (c–f) tests, representing multiple cognitive functions, were conducted sequentially. (a) The total number of arm entries was not significantly changed, indicating similar levels of motor and exploratory activity among the eight groups. (b) The percentage of spontaneous alternation was decreased in 5XFAD mice when compared with WT counterparts. (c) The average escape latency per day in the training day. (d) Number of crossings in the probe trial. (e) Time spent in target quadrant in the probe trial for each group. (f) Distance to the hidden platform per day in the training day. 3-month-old: $n = 15$ in each group; 7-month-old: $n = 12$ in each group; 11-month-old: $n = 10$ in each group; and 18-month-old: $n = 9$ in each group. Data were expressed as mean ± standard error. $^{*}P < 0.05$, $^{\dagger}P < 0.01$, $^{\ddagger}P < 0.001$, compared with age-matched WT mice; $^{\S}P < 0.05$, $^{\|}P < 0.01$, $^{\P}P < 0.001$, compared with the 3-month-old group of the same genotype. WT: Wild type.

Taken together, Aβ increased the p16 expression in neurons in a concentration- and time-dependent manner to some degree. These findings indicated that the arrest of cell cycle may contribute to the senescence of primary neurons.

## Discussion

In the present study, we screened and compared the expressions of cell cycle-related genes (*p53*, *p21*, *p16,* and cyclinD2) in the hippocampus from 5XFAD and WT mice, which demonstrated the profiles of CS and cognitive impairment of 5XFAD and WT mice in the whole life course. More importantly, we found that p16-positive neuronal cells obviously accumulated in pyramidal cells of the aged brains and markedly increased in 5XFAD mice. Meanwhile, the significantly upregulated p16 was negatively correlated with the cognitive performance of AD mice during the aging process, which may be associated with Aβ deposition in the cell microenvironment, indicating an accelerated CS in 5XFAD mice.

Up to date, no consensus has been reached with regard to the cellular localization of p16 in the hippocampus. Hence, we investigated the cell specificity of p16 upregulation by double immunofluorescence staining and found that p16 was mainly located in neuronal cells, with a marginal expression in astrocytes. This finding was consistent with the previous observations that p16 was co-localized with PHFs in AD brains[18] and that p16 was expressed in senescent astrocytes.[21,29]

Gene expression of *p16* mRNA was not changed at 1 month (before Aβ deposition), but increased sharply in the hippocampus of 5XFAD mice after 7 months, suggesting that p16 as a distinct senescent phenotype of CNS mature neurons can be considered as a pathological characteristic of AD. The increased p16 expression may be due to oxidative stress-induced damage to DNA.[30,31] With regard to the downstream signals of p16 (INK4a), p16 activates the pRB tumor suppressor, which silence certain pro-proliferative genes by heterochromatinization, thereby instituting a stringent arrest of cell proliferation.[2,32]

To further investigate the relationship between expression tendency of p53, p16, and cognitive changes during aging, the correlation analysis was conducted. The results revealed that p16, not p53, was negatively associated with the cognitive performances in both Y-maze and Morris water maze tests, despite a previous report that p53 was upregulated in AD.[16]

It is worth noticing that during normal brain aging, the aged WT mice also showed cognitive decline coupled with the upregulation of p16, whose mRNA and protein levels in the hippocampus were also negatively correlated with time spent in the target quadrant of Morris water maze test, suggesting that CS may participate in the physiological brain senescence, which resembles that of other organs.[33,34] However, compared with that of 5XFAD mice, the increase of p16 during normal aging was so sluggish and mild, even in the most aged mice, which formed a drastic contrast.

In the current study, oAβ enhanced the p16 expression, suggesting that in response to the neurotoxicity of Aβ, neurons trigger CS by p16 signaling pathway. Therefore, we proposed that in the AD context, constantly incremented

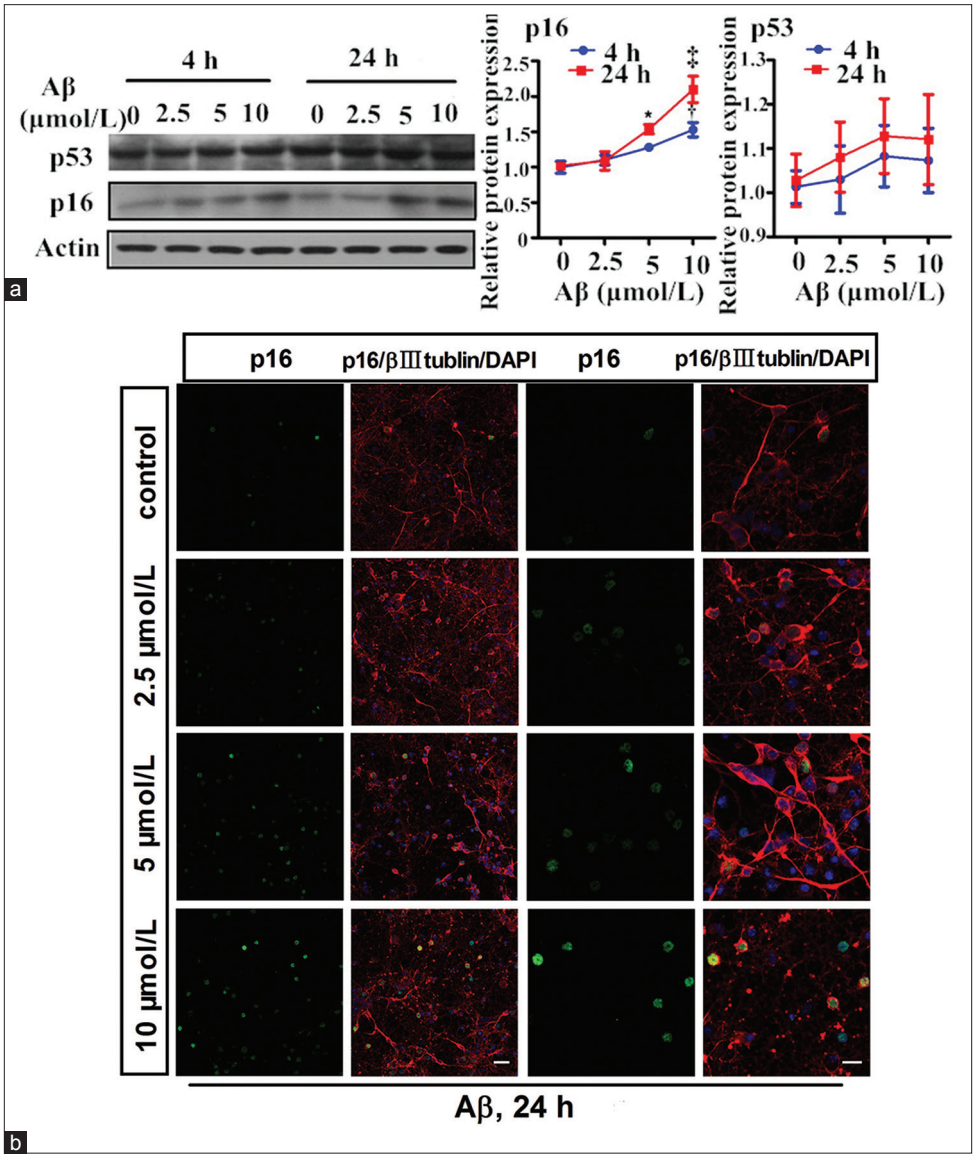


**Figure 4:** oAβ-induced p16 upregulation in neurons in a concentration- and time-dependent manner. (a) Western blotting analysis illustrated that oAβ increased p16 expression, but not p53 expression, in a concentration-dependent manner after 24 h exposure. The line graphs represented quantified results of p16 and p53, respectively, $n = 3$ in each group. p16 and p53 levels were normalized to control levels. $^{*}P < 0.05$, $^{\dagger}P < 0.01$, $^{\ddagger}P < 0.001$, compared with the vehicle group. (b) Double immunofluorescence staining showed the p16 (red) expression in cultured primary neurons after the treatment of different doses of oAβ for 24 h. βIII-tubulin (green) was co-stained as characterization of neurons. Cell nuclei were counterstained with DAPI, $n = 3$ in each group. Scale bar = 20 μm for the left side and scale bar = 10 μm for the right side. oAβ: Oligomeric amyloid β.

**Table 2: Pearson's correlation between senescent marker p16, p53 expression and cognitive performance in mice**

| Items | Spontaneous alteration | Number of crossings | Time spent in quadrant |
|---|---|---|---|
| p16 mRNA (WT) | –0.379 (0.164) | –0.387 (0.155) | –0.646 (0.009) |
| p16 protein (WT) | –0.490 (0.089) | –0.682 (0.010) | –0.754 (0.003) |
| p16 mRNA (5XFAD) | –0.591 (0.008) | –0.645 (0.003) | –0.551 (0.014) |
| p16 protein (5XFAD) | –0.767 (0.002) | –0.572 (0.041) | –0.737 (0.004) |
| p53 mRNA (WT) | –0.450 (0.123) | –0.073 (0.812) | –0.340 (0.256) |
| p53 protein (WT) | –0.442 (0.131) | –0.397 (0.180) | –0.363 (0.222) |
| p53 mRNA (5XFAD) | –0.047 (0.845) | –0.222 (0.347) | –0.096 (0.689) |
| p53 protein (5XFAD) | –0.173 (0.591) | –0.438 (0.154) | –0.464 (0.129) |

The data are shown as *r* (*P*). WT: Wild type; mRNA: Messenger RNA.

Aβ level may induce the upregulation of p16 in neurons. Meanwhile, Aβ treatment did not significantly interfere with p53, which was in line with the protein level of p53 *in vivo*. Of note, Aβ did not induce the senescence-associated beta-galactosidase activity in cultured neurons (data not shown), indicating that SA-β-gal was not required for neuronal senescence *in vitro*, although it was a classic CS biomarker.[35-37] This finding suggested a characteristic aging pattern of neuronal senescence, i.e., the expression of p16 instead of SA-β-gal *in vitro*.

Fortunately, a few studies have been carried out to show the underlying molecular mechanism of CS in aging-associated neurodegenerative diseases. A possible mechanism is that chronic inflammation, which is noted in the earliest stages of

the disease process, and senescence are mutually reinforcing each other, a state named as senescence-associated secretory phenotype.[2,38-40] In fact, normal aging is accompanied by a low-level, chronic inflammatory process. The mRNA level of pro-inflammatory mediators, such as interleukin (IL-1β), IL-6, and tumor necrosis factor-α has been shown to be elevated in normal aging, which was an early event in our AD mice (unpublished observation). Another possible mechanism is DNA damage response, including the formation of DNA damage foci (activated H2AX) and breaks in the double strands of DNA due to high reactive oxygen species production and oxidative damage.[31,41]

AD and normal brain aging process share common molecular changes, so it has been hypothesized that AD can be a form of accelerated brain aging and, in turn, exacerbates memory deficit, which indicate the culprit role of Aβ.[42,43] Aβ peptides aggravate the senescence of both CNS cells in AD and endothelial cells in cerebral amyloid angiopathy.[44] Thus, from this perspective, anti-aging molecules with antioxidant properties, such as sirtuins,[45,46] coenzyme Q10,[47] glutathione,[48] ginsenoside Rg1,[49] resveratrol,[50] and lifestyle impact, for instance, exercise[51] and drinking green tea, will present as potential and promising neuronal protectants for alleviating age-related cognitive decline.[52,53]

In summary, the current study found that CS due to the abnormalities of cell cycle-related genes may contribute to the cognitive deterioration in Aβ context, supporting the mitosis failure hypothesis in AD.[12] However, an important limitation of the present work was that we just demonstrated the correlation between p16 and cognition impairment, not a causal relationship on a macroscopic level during aging. More studies are enthusiastically anticipated to investigate the mechanism to clarify the senescence-associated biological process as well as possible interventions to delay aging and ultimately improve cognition impairment.


## Acknowledgments

We would like to thank teacher Hong-Zhi Huang from College of Foreign Languages of Fujian Medical University for the kindly help of text modifications and retouching of this paper.

## Financial support and sponsorship

This study was supported by grants from National Natural Science Foundation of China (No. 81200991 and No. 81571257), Fujian Provincial Natural Science Foundation (No. 2015J01398), Fujian Provincial New Century Excellent Talents Support Program, China (JA13131), and Young and Middle-aged Talent Training Key Project in Health System of Fujian Province (2014-ZQN-ZD-11).


## Conflicts of interest

There are no conflicts of interest.

## References


1. Querfurth HW, LaFerla FM. Alzheimer's disease. N Engl J Med 2010;362:329-44. doi: 10.1056/NEJMra0909142.
2. Campisi J. Aging, cellular senescence, and cancer. Annu Rev Physiol 2013;75:685-705. doi: 10.1146/annurev-physiol-030212-183653.
3. Deak F, Freeman WM, Ungvari Z, Csiszar A, Sonntag WE. Recent developments in understanding brain aging: Implications for Alzheimer's disease and vascular cognitive impairment. J Gerontol A Biol Sci Med Sci 2016;71:13-20. doi: 10.1093/gerona/glv206.
4. López-Otín C, Blasco MA, Partridge L, Serrano M, Kroemer G. The hallmarks of aging. Cell 2013;153:1194-217. doi: 10.1016/j.cell.2013.05.039.
5. Tacutu R, Budovsky A, Yanai H, Fraifeld VE. Molecular links between cellular senescence, longevity and age-related diseases – A systems biology perspective. Aging (Albany NY) 2011;3:1178-91. doi: 10.18632/aging.100413.
6. Campisi J, Andersen JK, Kapahi P, Melov S. Cellular senescence: A link between cancer and age-related degenerative disease? Semin Cancer Biol 2011;21:354-9. doi: 10.1016/j.semcancer.2011.09.001.
7. Campisi J. Cellular senescence: Putting the paradoxes in perspective. Curr Opin Genet Dev 2011;21:107-12. doi: 10.1016/j.gde.2010.10.005.
8. Kuilman T, Michaloglou C, Mooi WJ, Peeper DS. The essence of senescence. Genes Dev 2010;24:2463-79. doi: 10.1101/gad.1971610.
9. Zhan Y, Song C, Karlsson R, Tillander A, Reynolds CA, Pedersen NL, *et al.* Telomere length shortening and Alzheimer disease – A Mendelian Randomization Study. JAMA Neurol 2015;72:1202-3. doi: 10.1001/jamaneurol.2015.1513.
10. Mombach JC, Bugs CA, Chaouiya C. Modelling the onset of senescence at the G1/S cell cycle checkpoint. BMC Genomics 2014;15 Suppl 7:S7. doi: 10.1186/1471-2164-15-S7-S7.
11. Schmetsdorf S, Arnold E, Holzer M, Arendt T, Gärtner U. A putative role for cell cycle-related proteins in microtubule-based neuroplasticity. Eur J Neurosci 2009;29:1096-107. doi: 10.1111/j.1460-9568.2009.06661.x.
12. Esteras N, Bartolomé F, Alquézar C, Antequera D, Muñoz Ú, Carro E, *et al.* Altered cell cycle-related gene expression in brain and lymphocytes from a transgenic mouse model of Alzheimer's disease [amyloid precursor protein/presenilin 1 (PS1)]. Eur J Neurosci 2012;36:2609-18. doi: 10.1111/j.1460-9568.2012.08178.x.
13. Ueberham U, Arendt T. The expression of cell cycle proteins in neurons and its relevance for Alzheimer's disease. Curr Drug Targets CNS Neurol Disord 2005;4:293-306. doi: 10.2174/1568007054038175.
14. van Leeuwen LA, Hoozemans JJ. Physiological and pathophysiological functions of cell cycle proteins in post-mitotic neurons: Implications for Alzheimer's disease. Acta Neuropathol 2015;129:511-25. doi: 10.1007/s00401-015-1382-7.
15. Baker DJ, Wijshake T, Tchkonia T, LeBrasseur NK, Childs BG, van de Sluis B, *et al.* Clearance of p16Ink4a-positive senescent cells delays ageing-associated disorders. Nature 2011;479:232-6. doi: 10.1038/nature10600.
16. Hooper C, Meimaridou E, Tavassoli M, Melino G, Lovestone S, Killick R. p53 is upregulated in Alzheimer's disease and induces tau phosphorylation in HEK293a cells. Neurosci Lett 2007;418:34-7. doi: 10.1016/j.neulet.2007.03.026.
17. Arendt T, Rödel L, Gärtner U, Holzer M. Expression of the cyclin-dependent kinase inhibitor p16 in Alzheimer's disease. Neuroreport 1996;7:3047-9. doi: 10.1097/00001756-199611250-00050.
18. McShea A, Harris PL, Webster KR, Wahl AF, Smith MA. Abnormal expression of the cell cycle regulators P16 and CDK4 in Alzheimer's disease. Am J Pathol 1997;150:1933-9.
19. Molofsky AV, Slutsky SG, Joseph NM, He S, Pardal R, Krishnamurthy J, *et al.* Increasing p16INK4a expression decreases forebrain progenitors and neurogenesis during ageing. Nature 2006;443:448-52. doi: 10.1038/nature05091.
20. He N, Jin WL, Lok KH, Wang Y, Yin M, Wang ZJ. Amyloid-ß(1-42) oligomer accelerates senescence in adult hippocampal neural stem/progenitor cells via formylpeptide receptor 2. Cell Death Dis 2013;4:e924. doi: 10.1038/cddis.2013.437.
21. Bhat R, Crowe EP, Bitto A, Moh M, Katsetos CD, Garcia FU, *et al.* Astrocyte senescence as a component of Alzheimer's disease. PLoS One 2012;7:e45069. doi: 10.1371/journal.pone.0045069.
22. Gilissen EP, Leroy K, Yilmaz Z, Kövari E, Bouras C, Boom A, *et al.* A neuronal aging pattern unique to humans and common chimpanzees. Brain Struct Funct 2016;221:647-64. doi: 10.1007/

s00429-014-0931-5.
23. Campos PB, Paulsen BS, Rehen SK. Accelerating neuronal aging in *in vitro* model brain disorders: A focus on reactive oxygen species. Front Aging Neurosci 2014;6:292. doi: 10.3389/fnagi.2014.00292.
24. Oakley H, Cole SL, Logan S, Maus E, Shao P, Craft J, *et al.* Intraneuronal beta-amyloid aggregates, neurodegeneration, and neuron loss in transgenic mice with five familial Alzheimer's disease mutations: Potential factors in amyloid plaque formation. J Neurosci 2006;26:10129-40. doi: 10.1523/JNEUROSCI.1202-06.2006.
25. Zhang J, Yang L, Lin N, Pan X, Zhu Y, Chen X. Aging-related changes in RP3V kisspeptin neurons predate the reduced activation of GnRH neurons during the early reproductive decline in female mice. Neurobiol Aging 2014;35:655-68. doi: 10.1016/j.neurobiolaging.2013.08.038.
26. Zeng Y, Zhang J, Zhu Y, Zhang J, Shen H, Lu J, *et al.* Tripchlorolide improves cognitive deficits by reducing amyloid ß and upregulating synapse-related proteins in a transgenic model of Alzheimer's disease. J Neurochem 2015;133:38-52. doi: 10.1111/jnc.13056.
27. Morris R. Developments of a water-maze procedure for studying spatial learning in the rat. J Neurosci Methods 1984;11:47-60. doi: 10.1016/0165-0270(84)90007-4.
28. Pan XD, Zhu YG, Lin N, Zhang J, Ye QY, Huang HP, *et al.* Microglial phagocytosis induced by fibrillar ß-amyloid is attenuated by oligomeric ß-amyloid: Implications for Alzheimer's disease. Mol Neurodegener 2011;6:45. doi: 10.1186/1750-1326-6-45.
29. Bitto A, Sell C, Crowe E, Lorenzini A, Malaguti M, Hrelia S, *et al.* Stress-induced senescence in human and rodent astrocytes. Exp Cell Res 2010;316:2961-8. doi: 10.1016/j.yexcr.2010.06.021.
30. Burton DG, Faragher RG. Cellular senescence: From growth arrest to immunogenic conversion. Age (Dordr) 2015;37:27. doi: 10.1007/s11357-015-9764-2.
31. Suberbielle E, Sanchez PE, Kravitz AV, Wang X, Ho K, Eilertson K, *et al.* Physiologic brain activity causes DNA double-strand breaks in neurons, with exacerbation by amyloid-ß. Nat Neurosci 2013;16:613-21. doi: 10.1038/nn.3356.
32. LaPak KM, Burd CE. The molecular balancing act of p16(INK4a) in cancer and aging. Mol Cancer Res 2014;12:167-83. doi: 10.1158/1541-7786.MCR-13-0350.
33. Sikora E, Bielak-Zmijewska A, Mosieniak G. Cellular senescence in ageing, age-related disease and longevity. Curr Vasc Pharmacol 2014;12:698-706. doi: 10.2174/15701611116613121909404 5.
34. Howieson DB, Camicioli R, Quinn J, Silbert LC, Care B, Moore MM, *et al.* Natural history of cognitive decline in the old. Neurology 2003;60:1489-94. doi: 10.1212/01.wnl.0000063317.44167.5c.
35. Itahana K, Campisi J, Dimri GP. Methods to detect biomarkers of cellular senescence: The senescence-associated beta-galactosidase assay. Methods Mol Biol 2007;371:21-31. doi: 10.1007/978-1-59745-361-53.
36. Debacq-Chainiaux F, Erusalimsky JD, Campisi J, Toussaint O. Protocols to detect senescence-associated beta-galactosidase (SA-betagal) activity, a biomarker of senescent cells in culture and *in vivo*. Nat Protoc 2009;4:1798-806. doi: 10.1038/nprot.2009.191.
37. Lee BY, Han JA, Im JS, Morrone A, Johung K, Goodwin EC, *et al.* Senescence-associated beta-galactosidase is lysosomal beta-galactosidase. Aging Cell 2006;5:187-95. doi: 10.1111/j.1474-9726.2006.00199.x.
38. Tilstra JS, Robinson AR, Wang J, Gregg SQ, Clauson CL, Reay DP, *et al.* NF-κB inhibition delays DNA damage-induced senescence and aging in mice. J Clin Invest 2012;122:2601-12. doi: 10.1172/JCI45785.
39. Zhu Y, Armstrong JL, Tchkonia T, Kirkland JL. Cellular senescence and the senescent secretory phenotype in age-related chronic diseases. Curr Opin Clin Nutr Metab Care 2014;17:324-8. doi: 10.1097/MCO.0000000000000065.
40. Golde TE, Miller VM. Proteinopathy-induced neuronal senescence: A hypothesis for brain failure in Alzheimer's and other neurodegenerative diseases. Alzheimers Res Ther 2009;1:5. doi: 10.1186/alzrt5.
41. Wang C, Jurk D, Maddick M, Nelson G, Martin-Ruiz C, von Zglinicki T. DNA damage response and cellular senescence in tissues of aging mice. Aging Cell 2009;8:311-23. doi: 10.1111/j.1474-9726.2009.00481.x.
42. Villemagne VL, Pike KE, Chételat G, Ellis KA, Mulligan RS, Bourgeat P, *et al.* Longitudinal assessment of Aß and cognition in aging and Alzheimer disease. Ann Neurol 2011;69:181-92. doi: 10.1002/ana.22248.
43. Rentz DM, Locascio JJ, Becker JA, Moran EK, Eng E, Buckner RL, *et al.* Cognition, reserve, and amyloid deposition in normal aging. Ann Neurol 2010;67:353-64. doi: 10.1002/ana.21904.
44. Donnini S, Solito R, Cetti E, Corti F, Giachetti A, Carra S, *et al.* Abeta peptides accelerate the senescence of endothelial cells *in vitro* and *in vivo*, impairing angiogenesis. FASEB J 2010;24:2385-95. doi: 10.1096/fj.09-146456.
45. Santos L, Escande C, Denicola A. Potential modulation of sirtuins by oxidative stress. Oxid Med Cell Longev 2016;2016:9831825. doi: 10.1155/2016/9831825.
46. Bonda DJ, Lee HG, Camins A, Pallàs M, Casadesus G, Smith MA, *et al.* The sirtuin pathway in ageing and Alzheimer disease: Mechanistic and therapeutic considerations. Lancet Neurol 2011;10:275-9. doi: 10.1016/S1474-4422(11)70013-8.
47. Muta-Takada K, Terada T, Yamanishi H, Ashida Y, Inomata S, Nishiyama T, *et al.* Coenzyme Q10 protects against oxidative stress-induced cell death and enhances the synthesis of basement membrane components in dermal and epidermal cells. Biofactors 2009;35:435-41. doi: 10.1002/biof.56.
48. Homma T, Fujii J. Application of glutathione as anti-oxidative and anti-aging drugs. Curr Drug Metab 2015;16:560-71. doi: 10.2174/1389200216666151015114515.
49. Yang L, Zhang J, Zheng K, Shen H, Chen X. Long-term ginsenoside Rg1 supplementation improves age-related cognitive decline by promoting synaptic plasticity associated protein expression in C57BL/6J mice. J Gerontol A Biol Sci Med Sci 2014;69:282-94. doi: 10.1093/gerona/glt091.
50. Braidy N, Jugder BE, Poljak A, Jayasena T, Mansour H, Nabavi SM, *et al.* Resveratrol as a potential therapeutic candidate for the treatment and management of Alzheimer's disease. Curr Top Med Chem 2016;16:1951-60. doi: 10.2174/1568026616666160204121431.
51. Garatachea N, Pareja-Galeano H, Sanchis-Gomar F, Santos-Lozano A, Fiuza-Luces C, Morán M, *et al.* Exercise attenuates the major hallmarks of aging. Rejuvenation Res 2015;18:57-89. doi: 10.1089/rej.2014.1623.
52. Schmidt A, Hammann F, Wölnerhanssen B, Meyer-Gerspach AC, Drewe J, Beglinger C, *et al.* Green tea extract enhances parieto-frontal connectivity during working memory processing. Psychopharmacology (Berl) 2014;231:3879-88. doi: 10.1007/s00213-014-3526-1.
53. Afzal M, Safer AM, Menon M. Green tea polyphenols and their potential role in health and disease. Inflammopharmacology 2015;23:151-61. doi: 10.1007/s10787-015-0236-1.